STRUCTURAL BIOLOGY COMMUNICATIONS

ISSN 2053-230X

Purification, crystallization and preliminary X-ray analysis of the periplasmic haem-binding protein HutB from *Vibrio cholerae*

Shubhangi Agarwal, Maitree Biswas and Jhimli Dasgupta*

Department of Biotechnology, St Xavier's College, 30 Park Street, Kolkata 700 016, India. *Correspondence e-mail: jhimlidasgupta@yahoo.com

Received 22 January 2015
Accepted 21 February 2015

Edited by M. L. Pusey, University of Alabama, USA

Keywords: *Vibrio cholerae*; iron uptake; periplasmic haem-binding protein; ABC transporter.

The mechanism of haem transport across the inner membrane of pathogenic bacteria is currently insufficiently understood at the molecular level and no information is available for this process in *Vibrio cholerae*. To obtain structural insights into the periplasmic haem-binding protein HutB from *V. cholerae* (VcHutB), which is involved in haem transport through the HutBCD haem-transport system, at the atomic level, VcHutB was cloned, overexpressed and crystallized using 1.6 *M* ammonium sulfate as a precipitant at pH 7.0. X-ray diffraction data were collected to 2.4 Å resolution on the RRCAT PX-BL-21 beamline at the Indus-2 synchrotron, Indore, India. The crystals belonged to space group $P4_32_12$, with unit-cell parameters $a = b = 62.88$, $c = 135.8$ Å. Matthews coefficient calculations indicated the presence of one monomer in the asymmetric unit, with an approximate solvent content of 45.02%. Molecular-replacement calculations with *Phaser* confirmed the presence of a monomer in the asymmetric unit.

1. Introduction

Vibrio cholerae, the causative agent of the diarrhoeal disease cholera (Faruque *et al.*, 1998; Kaper *et al.*, 1995), encodes a large number of nutrient-transport systems, reflecting the importance of these nutrients for its growth, survival and pathogenicity. In Gram-negative bacteria, the outer membrane forms a permeability barrier which restricts the passage of both nutrients and toxic environmental agents (Kadner, 1990; Moeck & Coulton, 1998). Therefore, most nutrients cross the outer membrane into the periplasmic space by diffusion through porins, while larger nutrients are transported into the periplasm *via* specific high-affinity active-transport systems. Transport of the essential nutrients through the periplasm and across the inner membrane is facilitated by a periplasmic binding protein-dependent ABC (ATP-binding cassette) transport system. In these systems, the periplasmic ligand-binding protein (PLBP) binds and delivers the ligand to the inner membrane permease (Oldham *et al.*, 2008).

Successful pathogenic bacteria must acquire one such essential nutrient, iron, from the host. Because the concentration of free iron in tissue is as low as 10^{-12} *M* (Clarke *et al.*, 2002), most pathogenic bacteria have developed elaborate mechanisms to obtain iron at concentrations sufficient for their growth. The main strategy for iron acquisition involves the synthesis and secretion of small iron-chelating molecules termed siderophores (Braun *et al.*, 1998; Byers & Arceneaux, 1998; Earhart, 1996). Additionally, numerous Gram-negative bacterial pathogens have developed a sophisticated mechanism for recruiting host haem iron (Eakanunkul *et al.*, 2005; Tong & Guo, 2007).

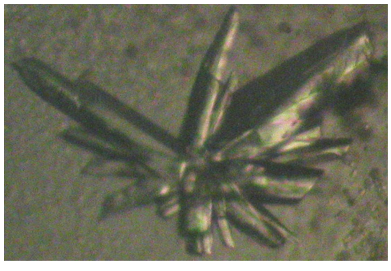

The first step of haem acquisition takes place through a TonB-dependent cell-surface receptor. Haem transport across the periplasmic space involves an ABC transporter system made up of a soluble PLBP, an inner membrane haem permease and an ATPase. Finally, upon crossing the inner membrane, the haem is broken down by haem oxygenase and iron is released into the cytosol. The mechanism of haem transport by haemin ABC transporters through the inner membrane is currently insufficiently understood at the molecular level. Ho *et al.* (2007) solved the crystal structures of two haem-binding PLBPs, ShuT from *Shigella dysenteriae* and PhuT from *Pseudomonas aeruginosa*, which share a common architecture with the haem binding in a narrow cleft between the N- and C-terminal binding domains (Ho *et al.*, 2007). A comparison of PhuT/ShuT with the vitamin B_{12} binding protein BtuF and the hydroxamic-type siderophore binding protein FhuD demonstrates that PhuT/ShuT more closely resemble BtuF, which reflects the closer similarity in ligands (haem and vitamin B_{12}) compared with the ligands of FhuD (Ho *et al.*, 2007). The periplasmic binding protein HmuT from *Yersinia pestis* (YpHmuT), however, binds two stacked haems in a central binding cleft that is larger than those of the homologous periplasmic haem-binding proteins ShuT and PhuT (Mattle *et al.*, 2010), pointing towards a variable mode of haem binding by PLBPs.

V. cholerae has multiple iron-acquisition systems, including the utilization of haem and haemoglobin, the synthesis and transport of the catechol-type siderophore vibriobactin and the transport of several exogenous siderophores such as enterobactin. Analysis of the *hut* genes indicated that *hutBCD*, which are predicted to encode a periplasmic binding protein (HutB), a cytoplasmic membrane permease (HutC) and an ATPase (HutD), are required to reconstitute the *V. cholerae* haem-transport system in *Escherichia coli* (Occhino *et al.*, 1998). However, mechanistic details of the transport of nutrients in *V. cholerae* are restricted to the structure of the vibriobactin binding protein ViuP in apo and holo forms (Li *et al.*, 2012), and the molecular mechanism of haem transport in *V. cholerae* is as yet unknown. Here, we report the cloning, overexpression, crystallization and preliminary X-ray crystallographic analysis of the periplasmic binding protein HutB (VcHutB) from *V. cholerae* O395 strain in the apo form.

2. Materials and methods

2.1. Cloning, overexpression and purification of VcHutB

The *hutB* gene was cloned into the kanamycin-resistant pET-28a(+) vector (Novagen) using specific primers (forward primer 5′-GGAATTCGCATATGCGGATCGTCAGTGCAG GAAGTGCAG-3′ and reverse primer 5′-CATTCGGGATCC-TCAGGGGTACAGCAGAGTTTGAATAC-3′). The primers were synthesized (NeuProCell) with NdeI and BamHI restriction-enzyme sites. Chromosomal DNA of *V. cholerae* strain O395, isolated using the protocol described in the Molecular Biology Laboratory Manual of UMBC (http://userpages.umbc.edu/~jwolf/method1.htm), was used as the template to amplify the region encoding *hutB*. The 762 bp *hutB* PCR amplicon and the pET-28a(+) vector were double-digested with the restriction enzymes NdeI and BamHI and the digested products were purified from 1.0% agarose gel using a gel-extraction kit (Invitrogen). These two double-digested DNA fragments were then ligated using T4 DNA ligase. The clones were selected appropriately using *E. coli* XL1-Blue cells with kanamycin resistance. The construct was verified by restriction-digestion analysis and DNA sequencing. VcHutB (residues 24–277 excluding the signal peptide; 254 amino acids) was then overexpressed in *E. coli* BL21(DE3) cells in the presence of the antibiotic kanamycin as a fusion protein with a 6×His tag at the N-terminus followed by a thrombin cleavage site (Fig. 1*a*).

For overexpression, 10 ml LB broth was inoculated with a single colony and was grown overnight at 310 K. 1 l LB broth was inoculated with 10 ml of the overnight culture and the culture was grown at 310 K until the OD_{600} reached 0.6. The cells were then induced with 1 m*M* isopropyl β-D-1-thiogalactopyranoside (IPTG). After induction at 310 K for 3 h, the cells were harvested at 4500*g* for 20 min and the pellet was resuspended in 7 ml ice-cold lysis buffer consisting of 50 m*M* Tris–HCl pH 7.0, 300 m*M* NaCl. Phenylmethylsulfonyl fluoride (final concentration of 1 m*M*) and 1 mg ml^{-1} lysozyme were added to the resuspended solution and the cells

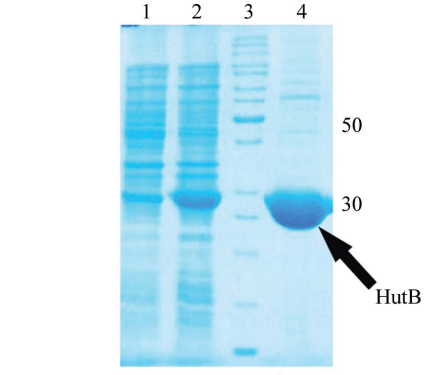

(*a*)

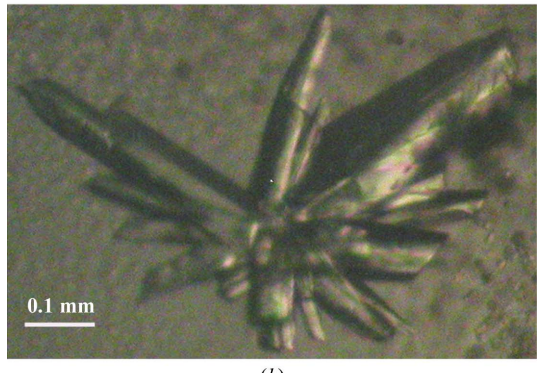

(*b*)

Figure 1
(*a*) 12% SDS–PAGE: lanes 1 and 2, uninduced and induced expression of 6×His-tagged VcHutB, respectively; lane 3, molecular-weight markers (labelled in kDa); lane 4, purified 6×His-tagged VcHutB. (*b*) Crystals of VcHutB grown in the presence of precipitant solution consisting of 1.6 *M* ammonium sulfate, 0.1 *M* HEPES pH 7.0.

Table 1
Data-collection and data-processing parameters.

Values in parentheses are for the outermost resolution shell.

Beamline	PX-BL-21, Indus-2
Wavelength (Å)	0.98
Oscillation (°)	1
No. of frames	132
Space group	$P4_32_12$
Unit-cell parameters (Å)	$a = b = 62.88$, $c = 135.8$
Resolution (Å)	37.0–2.4 (2.49–2.40)
No. of molecules in asymmetric unit	1
Mathews coefficient V_M (Å^3 Da^{-1})	2.24
Solvent content (%)	45.02
No. of observations	108572 (10718)
No. of unique reflections	11192 (1134)
Multiplicity	9.7 (9.5)
Mosaicity (°)	0.40
Completeness (%)	99.2 (97.5)
R_{merge}† (%)	6.1 (71.7)
Average $I/\sigma(I)$	29.9 (3.3)

† $R_{merge} = \sum_{hkl}\sum_i |I_i(hkl) - \langle I(hkl)\rangle| / \sum_{hkl}\sum_i I_i(hkl)$, where $I_i(hkl)$ is the observed intensity of the ith measurement of reflection hkl and $\langle I(hkl)\rangle$ is the mean intensity of reflection hkl calculated after scaling.

were lysed by sonication on ice. The cell lysate was then centrifuged (12 000*g* for 50 min) at 277 K and the supernatant was collected. Ni^{2+}–NTA (Qiagen) resin was equilibrated with the lysis buffer and the supernatant containing 6×His-tagged VcHutB was immobilized on the resin for Ni^{2+}–NTA-based immobilized metal-ion affinity chromatography. The resin was washed with wash buffers consisting of the components of the lysis buffer with increasing concentrations of imidazole (5 and 10 m*M*) and the 6×His-tagged VcHutB was eluted with elution buffer with an imidazole concentration of 150 m*M*. The purity of the eluted fractions was checked using 12% SDS–PAGE and the fractions were found to be nearly homogeneous. The eluted protein was dialyzed against Tris buffer consisting of 50 m*M* Tris–HCl pH 7.0, 300 m*M* NaCl and concentrated using an Amicon Ultra centrifugation unit (molecular-weight cutoff 10 kDa). The homogeneity of the purified protein was checked using 12% SDS–PAGE (Fig. 1*a*).

2.2. Crystallization

For crystallization, VcHutB was concentrated to 25 mg ml^{-1} using an Amicon Ultra centrifugation unit (molecular-weight cutoff 10 kDa) in buffer consisting of 50 m*M* Tris–HCl pH 7.0, 300 m*M* NaCl. The concentration of the protein was measured spectrophotometrically using a calculated extinction coefficient of 4470 M^{-1} cm^{-1}. Initial crystallization trials were performed by the hanging-drop vapour-diffusion method in 24-well crystallization trays (Hampton Research, Laguna Niguel, California, USA) using Grid Screen PEG 6000, Grid Screen Ammonium Sulfate, Crystal Screen (Jancarik & Kim, 1991) and Crystal Screen 2 from Hampton Research. Typically, 2 µl of protein solution was mixed with an equal volume of the screening solution and equilibrated against 600 µl of the latter. Initially, tiny crystals were observed in the presence of 20% PEG 6000 at pH 6.0 (a condition from Grid Screen PEG 6000) and 1.6 *M* ammonium sulfate pH 7.0 incubated at 293 K for two to three weeks. These crystallization conditions were further optimized. Finally, equilibration of a mixture of 3 µl protein solution with 2 µl precipitant solution consisting of 0.8 *M* ammonium sulfate, 0.1 *M* HEPES pH 7.0 against a reservoir solution consisting of 500 µl 1.6 *M* ammonium sulfate, 0.1 *M* HEPES pH 7.0 at 293 K for 21 d produced diffraction-quality crystals with a longest dimension of 0.4 mm (Fig. 1*b*).

2.3. Data collection and processing

Crystals of VcHutB were looped out using 0.4 mm LithoLoops (Molecular Dimensions), soaked in cryoprotectant consisting of 25%(*v*/*v*) glycerol, 1 *M* ammonium sulfate, 0.1 *M* HEPES pH 7.0, 150 m*M* NaCl and immediately flash-cooled in liquid nitrogen. The quality of the crystals was judged and the cooling conditions were optimized using a MAR Research image-plate detector (345 mm) and Cu $K\alpha$ radiation generated by a Bruker–Nonius FR591 rotating-anode generator equipped with Osmic MaxFlux confocal optics. Diffraction images were then collected from a cryocooled crystal (100 K) using a MAR225 CCD (Rayonix) detector on the RRCAT PX-BL-21 beamline at the Indus-2 synchrotron, Indore, India with an oscillation range of 1°. A total of 360 images were collected. The data were indexed and integrated using *XDS* (Kabsch, 2010) and subsequently scaled using *AIMLESS* from *CCP*4 (Winn *et al.*, 2011). Data-collection and processing parameters are given in Table 1.

3. Results

The crystals of VcHutB were of good quality and diffraction data were collected to 2.4 Å resolution. Although the R_{merge} in

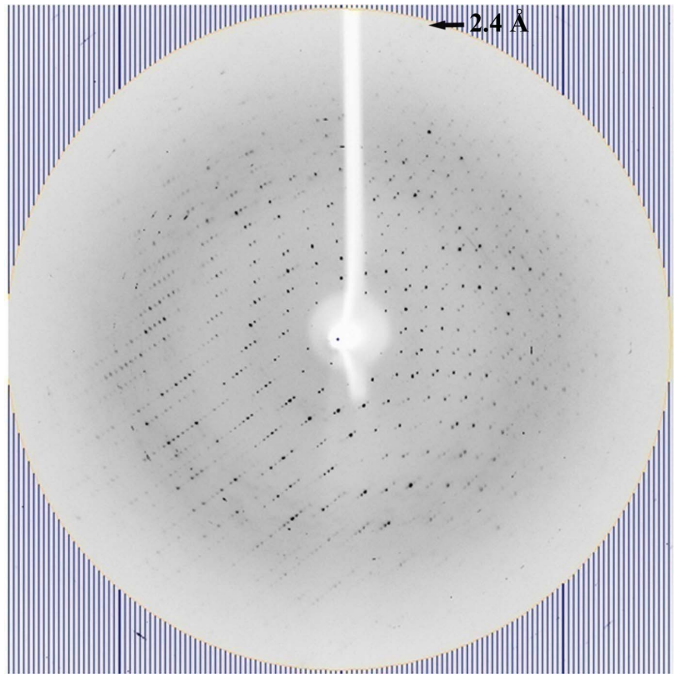

Figure 2
X-ray diffraction image of the VcHutB. The crystal diffracted to 2.4 Å resolution.

the highest resolution bin was 71.7%, the $\langle I/\sigma(I)\rangle$ and the completeness in the highest resolution bin were 3.3 and 97.5%, respectively; therefore, the data were processed to 2.4 Å resolution (Table 1). A typical diffraction image is shown in Fig. 2.

The VcHutB crystals belonged to the orthorhombic crystal system, with unit-cell parameters $a = b = 62.88$, $c = 135.8$ Å (Table 1). Calculation of the Matthews coefficient indicated the most probable presence of only one molecule (considering the molecular weight of 30 kDa) in the asymmetric unit, with a V_M (Matthews, 1968) of 2.24 Å Da^{-1} and a solvent content of 45.02%.

The initial phases were obtained by molecular replacement (MR) using *Phaser* (McCoy *et al.*, 2007). A *BLAST* search with the sequence of VcHutB against the PDB showed 32, 34 and 37% sequence identity to the haem-binding PLBPs ShuT from *S. dysenteriae*, PhuT from *P. aeruginosa* and HmuT from *Y. pestis*, respectively. Despite this, the coordinates of chain *A* of ShuT from *S. dysenteriae* in the apo form (PDB entry 2rg7; Ho *et al.*, 2007) produced an acceptable solution in MR. Before proceeding with the MR calculations, waters were deleted from the coordinates of the search model and the mismatched residues were mutated to alanine. One molecule of this modified search model in the asymmetric unit produced a rotation-function *Z*-score (RFZ) of 4.2, a translation-function *Z*-score (TFZ) of 10.0 and a convincing log-likelihood gain (LLG) of 88.0 in space group $P4_32_12$ using data between 37.0 and 2.4 Å resolution. Interestingly, a search model consisting of the coordinates of the apo PLBP HmuT from *Y. pestis* did not produce any convincing solution. Initial structure refinement was carried out using *PHENIX* (Adams *et al.*, 2010), which resulted in a model with an R_{work} of 40.0% and an R_{free} of 46.9%. The $2F_o - F_c$ map calculated with this refined model was of good quality and overlaid properly with the model. Further model building and structure refinement are in progress. Detailed structural analysis of VcHutB will provide further insights into the mechanism of haem transport in pathogenic bacteria.

Acknowledgements

We are extremely grateful to the PX-BL-21 beamline scientists Dr R. Makde, Dr B. Ghosh and Mr A. Kumar of RRCAT, Indore, India for helping us to collect the diffraction data. We are also very grateful to Professor Udayaditya Sen of SINP, Kolkata for his help and suggestions. SA is grateful to Sanjay Dey of JD's laboratory at St Xavier's College, Kolkata for his help and suggestions during the experiments. We are grateful to Dr J. Felix Raj SJ, Principal, St Xavier's College, Kolkata for his encouragement and constant support. This work was supported by DAE (BRNS) grant No. 2013/37B/26/BRNS from the Government of India.

References

Adams, P. D. *et al.* (2010). *Acta Cryst.* D**66**, 213–221.
Braun, V., Hantke, K. & Köster, W. (1998). *Met. Ions Biol. Syst.* **35**, 67–145.
Byers, B. R. & Arceneaux, J. E. (1998). *Met. Ions Biol. Syst.* **35**, 37–66.
Clarke, T. E., Braun, V., Winkelmann, G., Tari, L. W. & Vogel, H. J. (2002). *J. Biol. Chem.* **277**, 13966–13972.
Eakanunkul, S., Lukat-Rodgers, G. S., Sumithran, S., Ghosh, A., Rodgers, K. R., Dawson, J. H. & Wilks, A. (2005). *Biochemistry*, **44**, 13179–13191.
Earhart, C. F. (1996). *Escherichia Coli and Salmonella: Cellular and Molecular Biology*, 2nd ed., Vol. 1. edited by F. C. Neidhardt, R. Curtiss III, J. L. Ingraham, E. C. C. Lin, K. B. Low, B. Magasanik, W. S. Reznikoff, M. Riley, M. Schaechter & H. E. Umbarger, pp. 1075–1090. Washington DC: ASM Press.
Faruque, S. M., Albert, M. J. & Mekalanos, J. J. (1998). *Microbiol. Mol. Biol. Rev.* **62**, 1301–1314.
Ho, W. W., Li, H., Eakanunkul, S., Tong, Y., Wilks, A., Guo, M. & Poulos, T. L. (2007). *J. Biol. Chem.* **282**, 35796–35802.
Jancarik, J. & Kim, S.-H. (1991). *J. Appl. Cryst.* **24**, 409–411.
Kabsch, W. (2010). *Acta Cryst.* D**66**, 125–132.
Kadner, R. J. (1990). *Mol. Microbiol.* **4**, 2027–2033.
Kaper, J. B., Morris, J. G. & Levine, M. M. (1995). *Clin. Microbiol. Rev.* **8**, 48–86.
Li, N., Zhang, C., Li, B., Liu, X., Huang, Y., Xu, S. & Gu, L. (2012). *J. Biol. Chem.* **287**, 8912–8919.
Matthews, B. W. (1968). *J. Mol. Biol.* **33**, 491–497.
Mattle, D., Zeltina, A., Woo, J. S., Goetz, B. A. & Locher, K. P. (2010). *J. Mol. Biol.* **404**, 220–231.
McCoy, A. J., Grosse-Kunstleve, R. W., Adams, P. D., Winn, M. D., Storoni, L. C. & Read, R. J. (2007). *J. Appl. Cryst.* **40**, 658–674.
Moeck, G. S. & Coulton, J. W. (1998). *Mol. Microbiol.* **28**, 675–681.
Occhino, D. A., Wyckoff, E. E., Henderson, D. P., Wrona, T. J. & Payne, S. M. (1998). *Mol. Microbiol.* **29**, 1493–1507.
Oldham, M. L., Davidson, A. L. & Chen, J. (2008). *Curr. Opin. Struct. Biol.* **18**, 726–733.
Tong, Y. & Guo, M. (2007). *J. Biol. Inorg. Chem.* **12**, 735–750.
Winn, M. D. *et al.* (2011). *Acta Cryst.* D**67**, 235–242.